Commun. Comput. Phys.
doi: 10.4208/cicp.OA-2023-0280

Vol. **36**, No. 1, pp. 133-159
July 2024

Optimal Error Estimates of a Discontinuous Galerkin Method for Stochastic Allen-Cahn Equation Driven by Multiplicative Noise

Xu Yang[1], Weidong Zhao[2] and Wenju Zhao[2,*]

[1] *School of Mathematics, China University of Mining and Technology, Xuzhou, Jiangsu 221116, China.*
[2] *School of Mathematics, Shandong University, Jinan, Shandong 250100, China.*

Received 25 October 2023; Accepted (in revised version) 21 April 2024

Abstract. In this paper, we develop and analyze an efficient discontinuous Galerkin method for stochastic Allen-Cahn equation driven by multiplicative noise. The proposed method is realized by symmetric interior penalty discontinuous Galerkin finite element method for space domain and implicit Euler method for time domain. Several new estimates and techniques are developed. Under some suitable regularity assumptions, we rigorously establish strong convergence results for the proposed fully discrete numerical scheme and obtain optimal convergence rates in both space and time. Numerical experiments are also carried out to validate our theoretical results and demonstrate the effectiveness of the proposed method.

AMS subject classifications: 60H15, 60H35, 65C30, 65M60

Key words: Stochastic Allen-Cahn equation, strong convergence, discontinuous Galerkin method, variational solution, multiplicative noise.

1 Introduction

In this paper, we consider strong approximation for the Itô type Allen-Cahn equation with multiplicative noise of the form

$$\mathrm{d}u + Au\,\mathrm{d}t = f(u)\,\mathrm{d}t + g(u)\,\mathrm{d}W \quad \text{in } D\times(0,T], \tag{1.1}$$

$$\frac{\partial u}{\partial \mathbf{n}} = 0 \quad \text{on } \partial D\times[0,T], \tag{1.2}$$

$$u = u_0 \quad \text{in } D\times\{t=0\}. \tag{1.3}$$

*Corresponding author. *Email addresses:* xuyang96@cumt.edu.cn (X. Yang), wdzhao@sdu.edu.cn (W. Zhao), zhaowj@sdu.edu.cn (W. Zhao)

Here T is a fixed positive time instant, D is a bounded convex domain in $\mathbb{R}^d$, $d=1,2,3$, with polygonal boundary ∂D, $\mathbf{n}$ denotes the unit outward normal vector to the boundary ∂D, the operator A denotes the linear elliptic operator defined by $Au:=-\Delta u$, $f\colon \mathbb{R}\to\mathbb{R}$ is given by $f(u):=\frac{1}{\epsilon^2}(u-u^3)$ with parameter ϵ the interfacial width, $g\colon \mathbb{R}\to\mathbb{R}$ is an appropriate regular function which will be specified in the next section, and the driving noise W is a standard Wiener process defined on a complete probability space $(\Omega,\mathcal{F},\mathbb{P})$ with normal filtration $\mathbb{F}=\{\mathcal{F}_t\}_{0\le t\le T}$. For the sake of notational simplicity, we focus our discussion on the one dimensional noise case and it is straightforward to generalize the analysis below to the multidimensional noise cases.

The deterministic Allen-Cahn equation was first introduced by Allen and Cahn in [1] to describe the motion of anti-phase boundaries of a binary alloy at a fixed temperature. Since then, as a fundamental tool, Allen-Cahn equation plays an important role in many complicated moving interface problems such as material science, fluid dynamics, image analysis and mean curvature flow [27]. Frequently, due to the presence of external perturbations, lack of information, uncertainty in the measurements, and incomplete knowledge of certain physical parameters, a stochastic noise is usually added in the model to make the description of the system more realistic, which results in the stochastic Allen-Cahn equation (SAC). Note that sharing the same structure with the deterministic case, the model (1.1) admits superlinearly growing coefficient and in general it can not be solved explicitly. In recent years, the construction and numerical analysis of efficient approximation schemes for stochastic Allen-Cahn equation have begun to attract the attention of many researchers and plenty of interesting numerical methods have been developed, analyzed and tested, see e.g. [3–5,9,17,28,29,37,38,41,45] and the references therein. However, most of the aforementioned works have considered the additive noise case, where the stochastic convolution plays a key role in the numerical analysis. In comparison with large amounts of numerical studies of stochastic Allen-Cahn equation with additive noise, the numerical studies of multiplicative noise driving stochastic Allen-Cahn equation are still very limited (see e.g. [21,30,37,39]).

Discontinuous Galerkin (DG) methods are a class of finite element methods with the basis functions which can be completely discontinuous [16]. DG methods are eligible for high order schemes in space and flexible of parallel implementation of handling the complex problem, which have been widely used to solve deterministic partial differential equations (PDEs). And we refer to the books [16, 18, 19, 42] for more details on the development of DG methods in all aspects including algorithm design, analysis, implementation and applications. As far as the stochastic cases are concerned, DG methods for stochastic partial differential equations (SPDEs) can inherit the advantages of their counterparts for deterministic PDEs and they are good choices to solve SPDEs with sharp feature. For this reason, recently, many researchers turn their attentions to working in the design and analysis of DG methods for SPDEs. A symmetric interior penalty DG and local DG for SPDEs are proposed and investigated in [34,46]. Discontinuous Galerkin methods for stochastic wave equations, Helmholtz equation, conservation laws and Kdv equations are investigated in [2,10,11,26,32,33]. Mean-square convergence analysis of a symplectic

local discontinuous Galerkin method applied to stochastic linear Schrödinger equation is carried out in [13]. Discontinuous Galerkin methods for the stochastic Maxwell equations are considered in [12, 43, 44]. Discontinuous Galerkin methods for the stochastic Cahn–Hilliard equation are studied in [31, 47], etc.

Our primary objective of this paper is to study the strong convergence of a fully discrete numerical method for multiplicative noise driving stochastic Allen-Cahn equation. To be precise, we will numerically solve model (1.1)-(1.3) with symmetric interior penalty discontinuous Galerkin (SIPG) finite element method in space and implicit Euler method in time. By overcoming a variety of technical difficulties in the numerical approximation of problem (1.1)-(1.3) caused by multiplicative nose, superlinear growth coefficients, and low time regularity of the solution, we provide rigorous error estimates with optimal strong convergence rates (see Theorem 4.1 in Section 4) for the proposed fully discrete scheme. In order to prove Theorem 4.1, we first establish some technical lemmas including time regularities in different form of the exact solution and stability properties of the proposed fully discrete approximation. Based on these established key lemmas, together with some classical error estimates from the finite element theory for deterministic PDEs, we eventually derive the strong approximation errors with optimal convergence rates in both space and time. As far as we are aware of, this is the first try to consider SIPG approximations for stochastic Allen-Cahn equation and obtain the optimal error estimates.

The rest of the paper is arranged as follows. In Section 2, we introduce some preliminaries and establish some regularity results of the solution. Section 3 is devoted to construct the proposed fully discrete numerical scheme. In Section 4, we first collect some well-known estimates and study the strong convergence of the proposed numerical scheme. The main result is also given. In Section 5, numerical experiments are carried out to validate our theoretical results. Finally, in Section 6 some concluding remarks are provided.

2 Preliminaries

Let $L^2(D)$ be the space of all square integrable functions equipped with the usual inner product $(\cdot,\cdot)$ and norm $\|\cdot\|$. Let $\kappa\geq 0$ be an arbitrary integer and $1\leq p\leq\infty$. We denote by $W^{\kappa,p}(D)$ the standard Sobolev space. For the case $p=2$, the space $W^{\kappa,2}(D)$ is a Hilbert space and we denote it by $H^\kappa(D)$, which is equipped with the norm $\|\cdot\|_{H^\kappa(D)}$ and the seminorm $|\cdot|_{H^\kappa(D)}=\|\nabla^\kappa\cdot\|_{L^2(D)}$. And obviously, $H^0(D)=L^2(D)$ and $|\cdot|_{H^0(D)}=\|\cdot\|_{L^2(D)}$. Let $C_b^\kappa(\mathbb{R})$ denote the space of bounded and κ-times continuously differentiable functions defined on $\mathbb{R}$ with bounded derivatives of all orders less than or equal to κ.

With a filtered probability space or stochastic basis $(\Omega,\mathcal{F},\mathbb{F},\mathbb{P})$ given in Section 1, we define $L^p(\Omega,\mathcal{F}_t;X),p\geq 1$ as the space of all $\mathcal{F}_t$-measurable X-valued random variables η satisfying $\mathbb{E}\left[\|\eta\|_X^p\right]<\infty$. Let $L_{\mathbb{F}}^p((0,T);X)$ denote the space of all $\mathbb{F}$-adapted X-valued

processes $\varphi=\{\varphi(t)\}_{t\in[0,T]}$ satisfying

$$\mathbb{E}\left[\int_0^T \|\varphi(t)\|_X^p \mathrm{d}t\right]<\infty.$$

Denote by $C_{\mathbb{F}}([0,T];L^2(\Omega,X))$ the space of all $\mathbb{F}$-adapted, mean square continuous, X-valued processes $\psi=\{\psi(t)\}_{t\in[0,T]}$ satisfying

$$\sup_{0\le t\le T}\mathbb{E}\left[\|\psi(t)\|_X^2\right]<\infty.$$

Let $L^2_{\mathbb{F}}(\Omega;C([0,T];X))$ be the subspace of $C_{\mathbb{F}}([0,T];L^2(\Omega,X))$ such that

$$\mathbb{E}\left[\sup_{0\le t\le T}\|\psi(t)\|_X^2\right]<\infty.$$

In the sequel, we impose the following condition on the function g in (1.1). The generic constant C will be used to denote generic positive constants independent of discretization parameters throughout the paper.

Assumption 2.1. Let $g\in C_b^\kappa(\mathbb{R})$ with $\kappa\ge 0$, and g is Lipschitz continuous and has linear growth, i.e., there exists a positive constant C such that for all $x,y\in\mathbb{R}$,

$$|g(x)-g(y)|\le C|x-y|. \tag{2.1}$$

And there exists a constant $M>0$ such that $|g(0)|\le M$.

Set $H:=L^2(D)$ and $V:=H^1(D)$. We identify H with its dual H^*, and denote by V^* the dual of V. Then we have the Gelfand triplet $V\hookrightarrow H\hookrightarrow V^*$. The duality pairing between V and V^* is denoted by $\langle\cdot,\cdot\rangle$. Obviously, the following relation holds:

$$\langle u,v\rangle=(u,v),\quad u\in H,\quad v\in V. \tag{2.2}$$

Define the operator $A\colon V\to V^*$ by

$$\langle Au,v\rangle=(\nabla u,\nabla v),\quad u,v\in V. \tag{2.3}$$

It is easy to see that there exists a positive constant C such that for all $w,w_1,w_2\in H$,

$$\big(f(w_1)-f(w_2),w_1-w_2\big)+\|g(w_1)-g(w_2)\|^2\le C\|w_1-w_2\|^2, \tag{2.4}$$

and

$$\|g(w)\|^2\le C\big(1+\|w\|^2\big). \tag{2.5}$$

Assumption 2.2 (Initial value)**.** The initial value u_0 is smooth enough, i.e., $u_0\in L^p(\Omega,\mathcal{F}_0;H^\kappa(D))$ with $p\ge 2$, $\kappa\ge 1$.

Definition 2.1. An $\mathbb{F}$-adapted process $u=\{u(t),t\in[0,T]\}$ is called a variational solution of the stochastic Allen-Cahn equation (1.1) if almost surly $u(t)\in V$ for almost every t and

$$(u(t),v)+\int_0^t\langle Au(s),v\rangle\,\mathrm{d}s=(u_0,v)+\int_0^t(f(u(s)),v)\,\mathrm{d}s+\int_0^t(g(u(s)),v)\,\mathrm{d}W(s), \tag{2.6}$$

holds for a.e. $\omega\in\Omega$, all $t\in[0,T]$, and all $v\in V$.

Next, we present some auxiliary results on existence and time regularity of solution to (1.1)-(1.3).

Theorem 2.1 ([14]). *Let Assumptions* 2.1–2.2 *hold. Then, the problem* (1.1)-(1.3) *admits a variational solution. Moreover, it holds*

$$\mathbb{E}\left[\sup_{0\le t\le T}\|u(t)\|^2\right]+\mathbb{E}\left[\int_0^T\|u(t)\|_V^2\,\mathrm{d}t\right]<\infty, \tag{2.7}$$

i.e., $u\in L^2_{\mathbb{F}}(\Omega;C([0,T];H))\cap L^2_{\mathbb{F}}((0,T);V)$.

Remark 2.1. From [22] and [39], let u be variational solution to the problem (1.1)-(1.3), then we have

$$\sup_{0\le t\le T}\mathbb{E}[\|u(t)\|^p]\bigvee\sup_{0\le t\le T}\mathbb{E}\left[\|u(t)\|^{10}_{L^{10}(D)}\right]<\infty,\quad p\ge1, \tag{2.8}$$

where $a\vee b:=\max\{a,b\}$.

The following lemmas deal with the time regularities of the solution in different norm.

Lemma 2.1. *Under the same assumptions of Theorem* 2.1*, let u be the variational solution of SAC* (1.1)*. If $g\in C_b^\kappa(\mathbb{R})$ and*

$$u\in C_{\mathbb{F}}\big([0,T];L^2(\Omega,H^\kappa(D))\big)\bigcap L^2_{\mathbb{F}}\big((0,T);H^{2+\kappa}(D)\big)$$

with $\kappa\ge0$ being integer, then we have

$$\mathbb{E}\left[|u(t)-u(s)|^2_{H^\kappa(D)}\right]\le C(t-s), \tag{2.9}$$

for $s,t\in[0,T]$ with $s<t$.

Proof. The proof is similar to the proof of Corollary 4.4 in [25] and Lemma 2.1 in [46]. Hence we omit it here. □

Lemma 2.2. *Let u be the variational solution of SAC* (1.1). *Suppose that*

$$u\in L^2_{\mathbb{F}}\big((0,T);H^{2+\kappa}(D)\big)\cap L^6_{\mathbb{F}}\big((0,T);H^{1+\kappa}(D)\big)$$

with $\kappa\geq 0$. Then it holds for $0\leq s<t\leq T$

$$|\mathbb{E}[u(t)-u(s)|\mathcal{F}_s]|^2_{H^\kappa(D)}\leq C(t-s)\mathbb{E}\left[\int_s^t \|u(\xi)\|^6_{H^{1+\kappa}(D)}+\|u(\xi)\|^2_{H^{2+\kappa}(D)}\,\mathrm{d}\xi|\mathcal{F}_s\right]. \tag{2.10}$$

Proof. We only prove the case $\kappa=0$ and the other cases can be proved in the same line. Due to the H^2–regularity, we have for $t>s$

$$u(t)-u(s)=\int_s^t Au(\xi)\,\mathrm{d}\xi+\int_s^t f(u(\xi))\,\mathrm{d}\xi+\int_s^t g(u(\xi))\,\mathrm{d}W(\xi). \tag{2.11}$$

Then taking the conditional mathematical expectation yields

$$\mathbb{E}[u(t)-u(s)|\mathcal{F}_s]=\mathbb{E}\left[\int_s^t Au(\xi)\,\mathrm{d}\xi|\mathcal{F}_s\right]+\mathbb{E}\left[\int_s^t f(u(\xi))\,\mathrm{d}\xi|\mathcal{F}_s\right], \tag{2.12}$$

from which we get

$$\|\mathbb{E}[u(t)-u(s)|\mathcal{F}_s]\|^2\leq 2\left\|\mathbb{E}\left[\int_s^t Au(\xi)\,\mathrm{d}\xi|\mathcal{F}_s\right]\right\|^2+2\left\|\mathbb{E}\left[\int_s^t f(u(\xi))\,\mathrm{d}\xi|\mathcal{F}_s\right]\right\|^2. \tag{2.13}$$

Using the Cauchy–Schwartz inequality and the Sobolev embedding $H^1(D)\hookrightarrow L^6(D)$ for $d\leq 3$ leads to

$$\begin{aligned}\|\mathbb{E}[u(t)-u(s)|\mathcal{F}_s]\|^2&\leq 2(t-s)\mathbb{E}\left[\int_s^t |u(\xi)|^2_{H^2(D)}\,\mathrm{d}\xi|\mathcal{F}_s\right]\\&\quad+2(t-s)\mathbb{E}\left[\int_s^t \left\|u(\xi)-u^3(\xi)\right\|^2\mathrm{d}\xi|\mathcal{F}_s\right]\\&\leq C(t-s)\mathbb{E}\left[\int_s^t \|u(\xi)\|^2_{H^2(D)}\,\mathrm{d}\xi|\mathcal{F}_s\right]\\&\quad+C(t-s)\mathbb{E}\left[\int_s^t \|u(\xi)\|^6_{L^6(D)}+\|u(\xi)\|^2\mathrm{d}\xi|\mathcal{F}_s\right]\\&\leq C(t-s)\mathbb{E}\left[\int_s^t \|u(\xi)\|^6_{H^1(D)}+\|u(\xi)\|^2_{H^2(D)}\,\mathrm{d}\xi|\mathcal{F}_s\right],\end{aligned} \tag{2.14}$$

which completes the proof. □

Using a similar argument as that in [21], we can derive the following lemma.

Lemma 2.3. *let u be the variational solution of SAC* (1.1). *Suppose that*

$$u\in C_{\mathbb{F}}\big([0,T];L^2(\Omega,H^2(D))\big).$$

Then, for $s,t\in[0,T]$ with $s<t$, we have

$$\mathbb{E}\left[\|f(u(t))-f(u(s))\|^2\right]\leq C(t-s), \tag{2.15}$$

where C is a positive constant.

3 Discontinuous Galerkin discretization

In this section, we propose a fully discrete discontinuous Galerkin scheme for (1.1)–(1.3). Let $\mathcal{T}_h$ with $h>0$ be a quasi-uniform triangulation of the space domain D such that $\overline{D}=\cup_{K\in\mathcal{T}_h}\overline{K}$. Let h_K denote the diameter of $K\in\mathcal{T}_h$ and $h:=\max_{K\in\mathcal{T}_h}h_K$. By ϱ_K we denote the largest d-dimensional ball inscribed into K. For a positive integer κ, we define a broken Sobolev space on $\mathcal{T}_h$ as

$$H^\kappa(\mathcal{T}_h):=\{v\in L^2(D);\, v|_K\in H^\kappa(K),\ \forall K\in\mathcal{T}_h\}$$

equipped with the broken Sobolev norm and seminorm:

$$\|v\|_{H^\kappa(\mathcal{T}_h)}=\left(\sum_{K\in\mathcal{T}_h}\|v\|^2_{H^\kappa(K)}\right)^{\frac{1}{2}},\quad |v|_{H^\kappa(\mathcal{T}_h)}=\left(\sum_{K\in\mathcal{T}_h}|v|^2_{H^\kappa(K)}\right)^{\frac{1}{2}}.$$

And clearly, $H^\kappa(D)\subset H^\kappa(\mathcal{T}_h)$. For any $K\in\mathcal{T}_h$, $P_r(K)$ denotes the set of all polynomials of degree at most $r\geq 1$ on the element K, and the DG finite element space S_h is defined as

$$S_h:=\{v\in L^2(D);\, v|_K\in P_r(K),\ \forall K\in\mathcal{T}_h\}. \tag{3.1}$$

Let $\mathcal{E}_h^I$ denote the set of all interior faces/edges of $\mathcal{T}_h$, $\mathcal{E}_h^B$ the set of all boundary faces/edges of $\mathcal{T}_h$, and $\mathcal{E}_h:=\mathcal{E}_h^I\cup\mathcal{E}_h^B$. Let $K,K'\in\mathcal{T}_h$ and e be an interior edge shared by two elements K and K', i.e., $e=\partial K\cap\partial K'$. Assume that the global labeling number of K is smaller than that of K'. We choose $\mathbf{n}_e:=\mathbf{n}_K|_e=-\mathbf{n}_{K'}|_e$ as the unit normal on e and define the following standard notations of jump and average across the face/edge e:

$$[[v]]:=v|_K-v|_{K'}\quad \text{on } e\in\mathcal{E}_h^I,$$
$$\{\{v\}\}:=\frac{1}{2}\big(v|_K+v|_{K'}\big)\quad \text{on } e\in\mathcal{E}_h^I,$$

for a scalar function v.

We now recall the following well-known result.

Lemma 3.1 ([18]). *If a function $v\in H^\kappa(\mathcal{T}_h)$ for $\kappa\geq 1$ belongs to $H^\kappa(D)$, then*

$$[[v]]=0,\quad \forall e\in\mathcal{E}_h^I, \tag{3.2}$$

and

$$\|v\|_{H^\kappa(\mathcal{T}_h)}=\|v\|_{H^\kappa(D)},\quad |v|_{H^\kappa(\mathcal{T}_h)}=|v|_{H^\kappa(D)}. \tag{3.3}$$

Now we define the DG bilinear form $a_h\colon H^\kappa(\mathcal{T}_h)\times H^\kappa(\mathcal{T}_h)\to\mathbb{R}$:

$$\begin{aligned}a_h(u,v)=&\sum_{K\in\mathcal{T}_h}\int_K\nabla u\cdot\nabla v\mathrm{d}x-\sum_{e\in\mathcal{E}_h^I}\int_e\{\{\nabla u\cdot\mathbf{n}_e\}\}[[v]]\mathrm{d}S\\&-\sum_{e\in\mathcal{E}_h^I}\int_e\{\{\nabla v\cdot\mathbf{n}_e\}\}[[u]]\mathrm{d}S+\sum_{e\in\mathcal{E}_h^I}\int_e\frac{\sigma}{h_e}[[u]][[v]]\mathrm{d}S,\end{aligned} \tag{3.4}$$

where the parameter $\sigma>0$ is called penalty parameter and h_e means the length of e in $2d$ and the area of e in $3d$. Now we define the so-called DG-norm

$$|||u|||=\left(\sum_{K\in\mathcal{T}_h}\|\nabla u\|^2_{L^2(K)}+\sum_{e\in\mathcal{E}_h^I}\frac{\sigma}{h_e}\|[[u]]\|^2_{L^2(e)}\right)^{\frac{1}{2}}. \tag{3.5}$$

3.1 Fully discrete scheme

In view of the definition of the weak solution and the bilinear form $a_h(\cdot,\cdot)$, we derive

$$(u(t),v)=(u_0,v)-\int_0^t a_h(u(s),v)\mathrm{d}s+\int_0^t(f(u(s)),v)\mathrm{d}s \tag{3.6}$$

$$+\int_0^t(g(u(s)),v)\mathrm{d}W(s),\quad \forall v\in H^s(\mathcal{T}_h),\quad t\in[0,T]. \tag{3.7}$$

Let $t_n=n\Delta t$ $(n=0,1,\cdots,\mathbb{M})$ be a uniform partition of $[0,T]$ with time step size $\Delta t=T/\mathbb{M}$. Denote by u_h^n the approximation of $u(t_n)$ at time t_n and define $\Delta W_n:=W(t_{n+1})-W(t_n)$. Based on (3.6), now we propose the space-time fully discrete scheme for SAC (1.1)-(1.3) as follows.

Scheme 3.1. Given an initial value $u_h^0=R_hu_0$, solve for u_h^{n+1}, $n=0,1,\cdots,\mathbb{M}-1$ such that for all $v_h\in S_h$

$$\begin{aligned}(u_h^{n+1},v_h)&=(u_h^n,v_h)-\int_{t_n}^{t_{n+1}}a_h(u_h^{n+1},v_h)\mathrm{d}s\\&\quad+\int_{t_n}^{t_{n+1}}(f(u_h^{n+1}),v_h))\mathrm{d}s+\int_{t_n}^{t_{n+1}}(g(u_h^n)),v_h)\mathrm{d}W(s)\\&=(u_h^n,v_h)-\Delta t a_h(u_h^{n+1},v_h)+\Delta t(f(u_h^{n+1}),v_h)\\&\quad+(v_h,g(u_h^n)\Delta W_n),\end{aligned} \tag{3.8}$$

where the definition of R_h is given in (4.3).

To analyze the well-posedness of Scheme 3.1, we introduce the following Browder fixed point theorem.

Lemma 3.2 (Browder fixed point theorem [8,23])**.** *Let $(E,(\cdot,\cdot))$ be a finite dimensional inner product space, $\|\cdot\|_E$ the associated norm, the mapping $\Pi:E\to E$ be continuous. Assume that $(\Pi z,z)\geq 0$ for all $z\in E$ with $\|z\|_E=\mu\geq 0$, then there exists a $z^*\in E$ such that $\Pi z^*=0$, $\|z^*\|_E\leq\mu$.*

Theorem 3.1. *Under the condition $\frac{\Delta t}{\epsilon^2}<1$, for all $\omega\in\Omega$, Scheme* 3.1 *is solvable.*

Proof. Referring to [8], let us fix $\omega\in\Omega$ and suppose that $u_h^k(\omega)$, $k=1,2,\cdots,n$ have been determined. We introduce the mapping $\Pi^\omega:S_h\to S_h$ defined by

$$\begin{aligned}(\Pi^\omega w_h,v_h)=&(w_h,v_h)-(u_h^n(\omega),v_h)+\Delta t a_h(w_h,v_h)\\&-\Delta t(f(w_h),v_h)-(v_h,g(u_h^n(\omega))\Delta W_n(\omega)),\quad\forall v_h\in S_h.\end{aligned} \tag{3.9}$$

Following Lemma 3.2, we have

$$\begin{aligned}(\Pi^{\omega}w_h,w_h)&=(w_h,w_h)-(u_h^n(\omega),w_h)+\Delta t a_h(w_h,w_h)\\&\quad-\Delta t(f(w_h),w_h)-(w_h,g(u_h^n(\omega))\Delta W_n(\omega))\\&\geq\|w_h\|^2-\|w_h\|\|u_h^n(\omega)\|+C_a\Delta t|||w_h|||^2\\&\quad+\frac{\Delta t}{\epsilon^2}(w_h^3-w_h,w_h)-\|w_h\|\|g_h(u_h^n(\omega))\Delta W_n(\omega)\|\\&\geq\left(\left(1-\frac{\Delta t}{\epsilon^2}\right)\|w_h\|-\|u_h^n(\omega)\|-\|g_h(u_h^n(\omega))\Delta W_n(\omega)\|\right)\|w_h\|.\end{aligned}$$

From [6,36], there exists a constant $C>0$ such that $\|v_h\|\leq C|||v_h|||$ for $v_h\in S_h$. By choosing $|||w_h|||=\mu\geq\frac{1}{C}\|w_h\|=\frac{\epsilon^2}{C(\epsilon^2-\Delta t)}(\|u_h^n(\omega)\|+\|g(u_h^n(\omega))\Delta W_n(\omega)\|)\geq 0$, we get $(\Pi^{\omega}w_h,w_h)\geq 0$ for all w_h with $|||w_h|||=\mu$. Hence $u_h^{n+1}(\omega)$ exists for all $\omega\in\Omega$. □

4 Strong convergence analysis

In this section, we are going to establish the optimal strong error estimates for the proposed fully discrete Scheme 3.1.

4.1 The main result

In this paper, the strong optimal error estimates are mainly considered for the proposed fully discrete Scheme 3.1. To start this section, we first present our main result in Theorem 4.1.

Theorem 4.1. *Let $u(t)$ and u_h^n, $n=0,1,2,\cdots,\mathbb{M}$ be the solutions of* (3.6) *and Scheme* 3.1*, respectively. Under the conditions given in Theorems* 3.1 *and* 4.2*, for a sufficient small $\Delta t>0$, there exists a constant C independent of h and Δt, such that*

$$\sup_{0\leq n\leq\mathbb{M}}\mathbb{E}\left[\|u_h^n-u(t_n)\|^2\right]+h^2C\mathbb{E}\left[\sum_{n=0}^{\mathbb{M}}|||u_h^n-u(t_n)|||^2\Delta t\right]\leq C\left(\Delta t+h^{2\min\{r+1,\kappa\}}\right).$$

4.2 Auxiliary theoretical techniques

We firstly collect some well-known estimates which are frequently used in our error analysis.

Lemma 4.1 (Continuity and coercivity [42])**.** *With a proper parameter $\sigma>0$, there exist positive constants $C>0$ and $C_a>0$ such that the DG bilinear form a_h has the following properties:*

$$a_h(u_h,v_h)\leq C|||u_h|||\,|||v_h|||,\quad u_h,v_h\in S_h,\tag{4.1}$$

$$a_h(v_h,v_h)\geq C_a|||v_h|||^2,\quad v_h\in S_h.\tag{4.2}$$

Next, we introduce the elliptic projection operator $R_h\colon H^1(\mathcal{T}_h)\to S_h$ defined by

$$a_h(R_h\varphi,\chi)=a_h(\varphi,\chi),\quad \forall\varphi\in H^1(\mathcal{T}_h),\quad \chi\in S_h. \tag{4.3}$$

Lemma 4.2 ([42]). *For $\kappa>3/2$, the following error estimates hold:*

$$|||u-R_hu|||\le Ch^{\min(r+1,\kappa)-1}\|u\|_{H^\kappa(\mathcal{T}_h)},\quad u\in H^\kappa(\mathcal{T}_h), \tag{4.4}$$

$$\|u-R_hu\|\le Ch^{\min(r+1,\kappa)}\|u\|_{H^\kappa(\mathcal{T}_h)},\quad u\in H^\kappa(D). \tag{4.5}$$

For $u\in H$, we define the L^2-projection operator $P_h\colon H\to S_h$ by

$$(P_hu,\chi)=(u,\chi),\quad \forall u\in H,\quad \forall\chi\in S_h. \tag{4.6}$$

Obviously, if $K\in\mathcal{T}_h$, then the function $P_hv|_K$ is the $L^2(K)$-projection of $v|_K$ on $P_r(K)$. Next, we cite some well-known error estimates for the L^2-projection operator P_h and we refer the readers to [7,15,20] for more details.

Lemma 4.3. *For the operator P_h, the standard error estimates read:*

$$\|P_hu-u\|\le Ch^{\min\{r+1,\kappa\}}\|u\|_{H^\kappa(D)}, \tag{4.7}$$

$$\|P_hu-u\|_{L^2(K)}\le Ch_K^{\min\{r+1,\kappa\}}\|u\|_{H^\kappa(K)}, \tag{4.8}$$

$$\|P_hu-u\|_{L^\infty(D)}\le Ch^{2-d/2}\|u\|_{H^2(D)} \tag{4.9}$$

for all $u\in H^\kappa(D)$.

Lemma 4.4 ([19]). *Assume the triangulations $\{\mathcal{T}_h\}_{h\in(0,h_0)}$,$h_0>0$ of the space domain D satisfy the shape-regularity condition, i.e., there exists a positive constant C such that*

$$\frac{h_K}{\varrho_k}\le C,\quad \forall K\in\mathcal{T}_h,\quad \forall h\in(0,h_0). \tag{4.10}$$

Then, there is a constant $C>0$ independent of v,h and K such that for $v\in H^1(K)$

$$\|v\|^2_{L^2(\partial K)}\le C\Big(\|v\|_{L^2(K)}|v|_{H^1(K)}+h_K^{-1}\|v\|^2_{L^2(K)}\Big),\quad \forall K\in\mathcal{T}_h. \tag{4.11}$$

Lemma 4.5 ([20]). *There exists a constant $C_I>0$ independent of v, h and K such that*

$$\|v\|_{L^\infty(K)}\le C_Ih_K^{-d/2}\|v\|_{L^2(K)},\quad \forall v\in S_h. \tag{4.12}$$

The following lemma is a generalised discrete Gronwall inequality.

Lemma 4.6 ([42]). *Let $\Delta t,B,C>0$ and let $\{a_n\},\{b_n\},\{c_n\}$ be sequences of nonnegative numbers satisfying*

$$\forall n\ge0,\qquad a_n+\Delta t\sum_{i=0}^n b_i\le B+C\Delta t\sum_{i=0}^n a_i+\Delta t\sum_{i=0}^n c_i. \tag{4.13}$$

Then, if $C\Delta t<1$,

$$\forall n\ge0,\qquad a_n+\Delta t\sum_{i=0}^n b_i\le e^{C(n+1)\Delta t}\left(B+\Delta t\sum_{i=0}^n c_i\right). \tag{4.14}$$

Define $\theta^n = u_h^n - R_h u(t_n)$, $\rho^n = u(t_n) - R_h u(t_n)$, so that the approximation error can be decomposed as

$$e^n = u_h^n - u(t_n) = \theta^n - \rho^n.$$

Our first step is to identify the error equation for the time evolution of θ^n. To the end, by subtracting (3.6) from (3.8), we infer that

$$\begin{aligned}
&(u_h^{n+1} - u(t_{n+1}), v_h) + \int_{t_n}^{t_{n+1}} a_h(u_h^{n+1} - u(t_{n+1}), v_h)\,\mathrm{d}s \\
&= (u_h^n - u(t_n), v_h) + \int_{t_n}^{t_{n+1}} (f(u_h^{n+1}) - f(R_h u(t_{n+1})), v_h)\,\mathrm{d}s \\
&\quad + \int_{t_n}^{t_{n+1}} (f(R_h u(t_{n+1})) - f(u(t_{n+1})), v_h)\,\mathrm{d}s + \Big(v_h, \int_{t_n}^{t_{n+1}} \big(g(u_h^n) - g(u(t_n))\big)\,\mathrm{d}W(s)\Big) \\
&\quad - \int_{t_n}^{t_{n+1}} a_h(u(t_{n+1}) - u(s), v_h)\,\mathrm{d}s + \int_{t_n}^{t_{n+1}} (f(u(t_{n+1})) - f(u(s)), v_h)\,\mathrm{d}s \\
&\quad + \Big(v_h, \int_{t_n}^{t_{n+1}} \big(g(u(t_n)) - g(u(s))\big)\,\mathrm{d}W(s)\Big), \quad \forall v_h \in S_h.
\end{aligned}$$

Using the definitions of θ^n and ρ^n leads to the error equation:

$$\begin{aligned}
&(\theta^{n+1} - \theta^n, v_h) + \int_{t_n}^{t_{n+1}} a_h(\theta^{n+1}, v_h)\,\mathrm{d}s \\
&= (\rho^{n+1} - \rho^n, v_h) + \int_{t_n}^{t_{n+1}} (f(u_h^{n+1}) - f(R_h u(t_{n+1})), v_h)\,\mathrm{d}s \\
&\quad + \int_{t_n}^{t_{n+1}} (f(R_h u(t_{n+1})) - f(u(t_{n+1})), v_h)\,\mathrm{d}s + \Big(v_h, \int_{t_n}^{t_{n+1}} \big(g(u_h^n) - g(u(t_n))\big)\,\mathrm{d}W(s)\Big) \\
&\quad - \int_{t_n}^{t_{n+1}} a_h(u(t_{n+1}) - u(s), v_h)\,\mathrm{d}s + \int_{t_n}^{t_{n+1}} (f(u(t_{n+1})) - f(u(s)), v_h)\,\mathrm{d}s \\
&\quad + \Big(v_h, \int_{t_n}^{t_{n+1}} \big(g(u(t_n)) - g(u(s))\big)\,\mathrm{d}W(s)\Big), \quad \forall v_h \in S_h.
\end{aligned} \tag{4.15}$$

4.3 Several key lemmas

In this subsection, we will establish several lemmas which will be used in our error estimates for Scheme 3.1.

Lemma 4.7 ([46]). *Suppose that* $\mathbb{E}\big[\|\psi\|_{H^1(D)}\big] < \infty$. *Then, the following relation holds*

$$\mathbb{E}[R_h \psi] = R_h \mathbb{E}[\psi]. \tag{4.16}$$

Lemma 4.8. *Suppose Assumptions* 2.1–2.2 *hold. Let* u *be the variational solution of SAC* (1.1). *Suppose that*

$$u \in C_{\mathbb{F}}\big([0,T]; L^6(\Omega, H^\kappa(D))\big)$$

with $\kappa \geq 2$. Then we have the following estimates

$$\begin{aligned}
&\frac{1}{2}\mathbb{E}\left[\|\theta^m\|^2\right]+\frac{1}{4}\mathbb{E}\left[\sum_{n=0}^{m-1}\|\theta^{n+1}-\theta^n\|^2\right]+C_a\mathbb{E}\left[\sum_{n=1}^{m}|||\theta^n|||^2\Delta t\right]\\
\leq& 2\mathbb{E}\left[\sum_{n=0}^{m-1}\|\rho^{n+1}-\rho^n\|^2\right]+\mathbb{E}\left[\sum_{n=0}^{m-1}\left(\mathbb{E}\left[\rho^{n+1}-\rho^n|\mathcal{F}_{t_n}\right],\theta^n\right)\right]\\
&+C\mathbb{E}\left[\sum_{n=0}^{m-1}\|\theta^{n+1}\|^2\Delta t\right]+C\mathbb{E}\left[\sum_{n=0}^{m-1}\|\rho^{n+1}\|^2\Delta t\right]\\
&+C\mathbb{E}\left[\sum_{n=0}^{m-1}\|\rho^{n}\|^2\Delta t\right]+C\sum_{n=0}^{m-1}\left(\mathbb{E}\left[\|\rho^{n+1}\|^6\right]\right)^{\frac{1}{3}}\Delta t\\
&+C\mathbb{E}\left[\sum_{n=0}^{m-1}\|\theta^{n}\|^2\Delta t\right]+\mathbb{E}\left[\sum_{n=0}^{m-1}\Xi^n\right],
\end{aligned}\tag{4.17}$$

where $\Xi^n:=\Xi_1^n+\Xi_2^n+\Xi_3^n$ with

$$\begin{aligned}
\Xi_1^n&=-\int_{t_n}^{t_{n+1}}a_h(u(t_{n+1})-u(s),\theta^{n+1})\,\mathrm{d}s,\\
\Xi_2^n&=\int_{t_n}^{t_{n+1}}(f(u(t_{n+1}))-f(u(s)),\theta^{n+1})\,\mathrm{d}s,\\
\Xi_3^n&=\left(\theta^{n+1},\int_{t_n}^{t_{n+1}}(g(u(t_n))-g(u(s)))\,\mathrm{d}W(s)\right).
\end{aligned}$$

Proof. By choosing $v_h=\theta^{n+1}$ in the error equation (4.15), we obtain

$$\begin{aligned}
&(\theta^{n+1}-\theta^n,\theta^{n+1})+\int_{t_n}^{t_{n+1}}a_h(\theta^{n+1},\theta^{n+1})\,\mathrm{d}s\\
=&(\rho^{n+1}-\rho^n,\theta^{n+1})+\int_{t_n}^{t_{n+1}}(f(u_h^{n+1})-f(R_hu(t_{n+1})),\theta^{n+1})\,\mathrm{d}s\\
&+\int_{t_n}^{t_{n+1}}(f(R_hu(t_{n+1}))-f(u(t_{n+1})),\theta^{n+1})\,\mathrm{d}s\\
&+\left(\theta^{n+1},\int_{t_n}^{t_{n+1}}\left(g(u_h^n)-g(u(t_n))\right)\mathrm{d}W(s)\right)\\
&-\int_{t_n}^{t_{n+1}}a_h(u(t_{n+1})-u(s),\theta^{n+1})\,\mathrm{d}s+\int_{t_n}^{t_{n+1}}(f(u(t_{n+1}))-f(u(s)),\theta^{n+1})\,\mathrm{d}s\\
&+\left(\theta^{n+1},\int_{t_n}^{t_{n+1}}\left(g(u(t_n))-g(u(s))\right)\mathrm{d}W(s)\right).
\end{aligned}\tag{4.18}$$

A straightforward algebraic calculation gives

$$(\theta^{n+1}-\theta^n,\theta^{n+1})=\frac{1}{2}\left(\|\theta^{n+1}\|^2-\|\theta^n\|^2\right)+\frac{1}{2}\|\theta^{n+1}-\theta^n\|^2.\tag{4.19}$$

It then follows that

$$\begin{aligned}
&\frac{1}{2}\left(\|\theta^{n+1}\|^2-\|\theta^n\|^2\right)+\frac{1}{2}\|\theta^{n+1}-\theta^n\|^2+a_h(\theta^{n+1},\theta^{n+1})\Delta t\\
=&(\rho^{n+1}-\rho^n,\theta^{n+1})+\Delta t(f(u_h^{n+1})-f(R_hu(t_{n+1})),\theta^{n+1})\\
&+\Delta t(f(R_hu(t_{n+1}))-f(u(t_{n+1})),\theta^{n+1})\\
&+(\theta^{n+1},(g(u_h^n)-g(u(t_n)))\Delta W_n)+\Xi^n.
\end{aligned}\tag{4.20}$$

Summing (4.20) from $n=0$ to $n=m-1$ with $m\leq\mathbb{M}$ yields

$$\begin{aligned}
&\frac{1}{2}\|\theta^m\|^2+\frac{1}{2}\sum_{n=0}^{m-1}\|\theta^{n+1}-\theta^n\|^2+C_a\sum_{n=1}^{m}|||\theta^n|||^2\Delta t\\
\leq&\sum_{n=0}^{m-1}(\rho^{n+1}-\rho^n,\theta^{n+1}-\theta^n)+\sum_{n=0}^{m-1}(\rho^{n+1}-\rho^n,\theta^n)\\
&+\sum_{n=0}^{m-1}\Delta t(f(u_h^{n+1})-f(R_hu(t_{n+1})),\theta^{n+1})\\
&+\sum_{n=0}^{m-1}\Delta t(f(R_hu(t_{n+1}))-f(u(t_{n+1})),\theta^{n+1})\\
&+\sum_{n=0}^{m-1}(\theta^{n+1}-\theta^n,(g(u_h^n)-g(u(t_n)))\Delta W_n)\\
&+\sum_{n=0}^{m-1}(\theta^n,(g(u_h^n)-g(u(t_n)))\Delta W_n)+\sum_{n=0}^{m-1}\Xi^n,
\end{aligned}\tag{4.21}$$

where the coercivity (4.2) of a_h has been used. Employing the Cauchy–Schwartz inequality and the Young inequality, we further get

$$\begin{aligned}
&\frac{1}{2}\|\theta^m\|^2+\frac{1}{2}\sum_{n=0}^{m-1}\|\theta^{n+1}-\theta^n\|^2+C_a\sum_{n=1}^{m}|||\theta^n|||^2\Delta t\\
\leq&2\sum_{n=0}^{m-1}\|\rho^{n+1}-\rho^n\|^2+\frac{1}{4}\sum_{n=0}^{m-1}\|\theta^{n+1}-\theta^n\|^2+\sum_{n=0}^{m-1}(\rho^{n+1}-\rho^n,\theta^n)+\sum_{n=0}^{m-1}\|\theta^{n+1}\|^2\Delta t\\
&+\sum_{n=0}^{m-1}\Delta t(f(u_h^{n+1})-f(R_hu(t_{n+1})),\theta^{n+1})+\sum_{n=0}^{m-1}\|f(R_hu(t_{n+1}))-f(u(t_{n+1}))\|^2\Delta t\\
&+2\sum_{n=0}^{m-1}\|(g(u_h^n)-g(u(t_n)))\Delta W_n\|^2+\sum_{n=0}^{m-1}(\theta^n,(g(u_h^n)-g(u(t_n)))\Delta W_n)+\sum_{n=0}^{m-1}\Xi^n.
\end{aligned}\tag{4.22}$$

Now, taking expectation and using the properties of conditional mathematical expecta-

tion and martingale give

$$\begin{aligned}
&\frac{1}{2}\mathbb{E}\left[\|\theta^m\|^2\right]+\frac{1}{4}\mathbb{E}\left[\sum_{n=0}^{m-1}\|\theta^{n+1}-\theta^n\|^2\right]+C\mathbb{E}\left[\sum_{n=1}^{m}|||\theta^n|||^2\Delta t\right]\\
\leq& 2\mathbb{E}\left[\sum_{n=0}^{m-1}\|\rho^{n+1}-\rho^n\|^2\right]+\mathbb{E}\left[\sum_{n=0}^{m-1}\Big(\mathbb{E}\big[\rho^{n+1}-\rho^n|\mathcal{F}_{t_n}\big],\theta^n\Big)\right]\\
&+\mathbb{E}\left[\sum_{n=0}^{m-1}\Delta t(f(u_h^{n+1})-f(R_hu(t_{n+1})),\theta^{n+1})\right]\\
&+\mathbb{E}\left[\sum_{n=0}^{m-1}\|f(R_hu(t_{n+1}))-f(u(t_{n+1}))\|^2\Delta t\right]+2\mathbb{E}\left[\sum_{n=0}^{m-1}\|(g(u_h^n)-g(u(t_n)))\Delta W_n\|^2\right]\\
&+C\mathbb{E}\left[\sum_{n=0}^{m-1}\|\theta^{n+1}\|^2\Delta t\right]+\mathbb{E}\left[\sum_{n=0}^{m-1}\Xi^n\right].
\end{aligned}\tag{4.23}$$

Together with (2.4), an application of the Itô isometry results in

$$\begin{aligned}
&\mathbb{E}\left[\sum_{n=0}^{m-1}\Delta t(f(u_h^{n+1})-f(R_hu(t_{n+1})),\theta^{n+1})\right]+\mathbb{E}\left[\sum_{n=0}^{m-1}\|(g(u_h^n)-g(u(t_n)))\Delta W_n\|^2\right]\\
=&\mathbb{E}\left[\sum_{n=0}^{m-1}\Delta t(f(u_h^{n+1})-f(R_hu(t_{n+1})),\theta^{n+1})\right]+\mathbb{E}\left[\sum_{n=0}^{m-1}\|(g(u_h^n)-g(u(t_n)))\|^2\Delta t\right]\\
\leq& C\mathbb{E}\left[\sum_{n=0}^{m-1}\|\theta^{n+1}\|^2\Delta t\right]+\mathbb{E}\left[\sum_{n=0}^{m-1}\Big(C\|\theta^n-\rho^n\|^2\Delta t\Big)\right]\\
\leq& C\mathbb{E}\left[\sum_{n=0}^{m}\|\rho^n\|^2\Delta t\right]+C\mathbb{E}\left[\sum_{n=0}^{m-1}\|\theta^n\|^2\Delta t\right]+C\mathbb{E}\left[\sum_{n=0}^{m-1}\|\theta^{n+1}\|^2\Delta t\right].
\end{aligned}\tag{4.24}$$

By virtue of the definition of f and Hölder's inequality, we arrive at

$$\begin{aligned}
&\mathbb{E}\left[\sum_{n=0}^{m-1}\|f(R_hu(t_{n+1}))-f(u(t_{n+1}))\|^2\Delta t\right]\\
=&\Delta t\sum_{n=0}^{m-1}\mathbb{E}\left[\left\|\rho^{n+1}\Big(u(t_{n+1})^2+u(t_{n+1})R_hu(t_{n+1})+(R_hu(t_{n+1}))^2-1\Big)\right\|^2\right]\\
\leq& C\Delta t\sum_{n=0}^{m-1}\mathbb{E}\left[\|u(t_{n+1})^2+u(t_{n+1})R_hu(t_{n+1})+(R_hu(t_{n+1}))^2-1\|_{L^\infty(D)}^2\|\rho^{n+1}\|^2\right]\\
\leq& C\Delta t\sum_{n=0}^{m-1}\Big(\mathbb{E}\big[\|u(t_{n+1})\|_{L^\infty(D)}^6+\|R_hu(t_{n+1})\|_{L^\infty(D)}^6+1\big]\Big)^{\frac{2}{3}}\Big(\mathbb{E}\big[\|\rho^{n+1}\|^6\big]\Big)^{\frac{1}{3}}\\
\leq& C\Delta t\sum_{n=0}^{m-1}\Big(\Phi(u)\Big)^{\frac{2}{3}}\Big(\mathbb{E}\big[\|\rho^{n+1}\|^6\big]\Big)^{\frac{1}{3}}
\end{aligned}$$

with

$$\Phi(u):=\mathbb{E}\Big[\|u(t_{n+1})\|^6_{L^\infty(D)}+\|R_hu(t_{n+1})-u(t_{n+1})\|^6_{L^\infty(D)}+1\Big].$$

With the aid of the triangle inequality and the Sobolev embedding $H^2(D)\hookrightarrow L^\infty(D)$ for $d\leq 3$, we derive

$$\begin{aligned}\Phi(u)\leq&\mathbb{E}\big[\|u(t_{n+1})\|^6_{L^\infty(D)}\big]+\mathbb{E}\left[\sup_{K\in\mathcal{T}_h}\|R_hu(t_{n+1})-P_hu(t_{n+1})\|^6_{L^\infty(K)}\right]\\&+\mathbb{E}\big[\|P_hu(t_{n+1})-u(t_{n+1})\|^6_{L^\infty(D)}\big]+1\\\leq&\mathbb{E}\big[\|u(t_{n+1})\|^6_{H^2(D)}\big]+\mathbb{E}\left[\sup_{K\in\mathcal{T}_h}\|R_hu(t_{n+1})-P_hu(t_{n+1})\|^6_{L^\infty(K)}\right]\\&+\mathbb{E}\big[\|P_hu(t_{n+1})-u(t_{n+1})\|^6_{L^\infty(D)}\big]+1.\end{aligned}\tag{4.25}$$

In view of Lemmas 4.2, 4.3 and 4.5, we further get

$$\begin{aligned}\Phi(u)\leq&\mathbb{E}\big[\|u(t_{n+1})\|^6_{H^2(D)}\big]+C\mathbb{E}\left[\sup_{K\in\mathcal{T}_h}h_K^{-3d}\|R_hu(t_{n+1})-P_hu(t_{n+1})\|^6_{L^2(K)}\right]\\&+\mathbb{E}\big[\|P_hu(t_{n+1})-u(t_{n+1})\|^6_{L^\infty(D)}\big]+1\\\leq&\mathbb{E}\big[\|u(t_{n+1})\|^6_{H^2(D)}\big]+C\mathbb{E}\left[\sup_{K\in\mathcal{T}_h}h_K^{-3d}\|R_hu(t_{n+1})-u(t_{n+1})\|^6_{L^2(K)}\right]\\&+C\mathbb{E}\left[\sup_{K\in\mathcal{T}_h}h_K^{-3d}\|P_hu(t_{n+1})-u(t_{n+1})\|^6_{L^2(K)}\right]\\&+\mathbb{E}\big[\|P_hu(t_{n+1})-u(t_{n+1})\|^6_{L^\infty(D)}\big]+1\\\leq&\mathbb{E}\big[\|u(t_{n+1})\|^6_{H^2(D)}\big]+C\mathbb{E}\left[\sup_{K\in\mathcal{T}_h}h_K^{-3d}h^{6\min(r+1,\kappa)}\|u(t_{n+1})\|^6_{H^\kappa(K)}\right]\\&+C\mathbb{E}\left[\sup_{K\in\mathcal{T}_h}h_K^{-3d}h^{6\min(r+1,\kappa)}\|u(t_{n+1})\|^6_{H^\kappa(K)}\right]\\&+Ch^{12-3d}\mathbb{E}\Big[\|u(t_{n+1})\|^6_{H^2(D)}\Big]+1\\\leq&\mathbb{E}\big[\|u(t_{n+1})\|^6_{H^2(D)}\big]+C\mathbb{E}\left[\sup_{K\in\mathcal{T}_h}\|u(t_{n+1})\|^6_{H^\kappa(K)}\right]\\&+Ch^{12-3d}\mathbb{E}\Big[\|u(t_{n+1})\|^6_{H^2(D)}\Big]+1\\\leq&C\mathbb{E}\big[\|u(t_{n+1})\|^6_{H^2(D)}\big]+C\mathbb{E}\big[\|u(t_{n+1})\|^6_{H^\kappa(D)}\big]+1<\infty.\end{aligned}\tag{4.26}$$

As a consequence, we have

$$\mathbb{E}\left[\sum_{n=0}^{m-1}\|f(R_hu(t_{n+1}))-f(u(t_{n+1}))\|^2\Delta t\right]\leq C\sum_{n=0}^{m-1}\Big(\mathbb{E}\big[\|\rho^{n+1}\|^6\big]\Big)^{\frac{1}{3}}\Delta t.\tag{4.27}$$

Substituting (4.24) and (4.27) into (4.23) ends the proof. □

Lemma 4.9. *Under the same conditions of Lemmas* 2.1 *and* 2.3*, there exist two positive numbers* ε_1 *and* ε_2 *such that*

$$\mathbb{E}\left[\sum_{n=0}^{m-1}\Xi^n\right]\leq C\Delta t+\varepsilon_1\mathbb{E}\left[\sum_{n=1}^{m}|||\theta^n|||^2\Delta t\right]+C\Delta t\mathbb{E}\left[\sum_{n=0}^{m-1}\|\theta^{n+1}\|^2\right]+\varepsilon_2\mathbb{E}\left[\sum_{n=0}^{m-1}\|\theta^{n+1}-\theta^n\|^2\right]. \tag{4.28}$$

Proof. Note that

$$\begin{aligned}\mathbb{E}\left[\sum_{n=0}^{m-1}\Xi^n\right]=&\mathbb{E}\left[\sum_{n=0}^{m-1}\Xi_1^n\right]+\mathbb{E}\left[\sum_{n=0}^{m-1}\Xi_2^n\right]+\mathbb{E}\left[\sum_{n=0}^{m-1}\Xi_3^n\right]\\:=&\mathcal{R}_1+\mathcal{R}_2+\mathcal{R}_3.\end{aligned}$$

By the same argument as that in Lemma 4.7 of [46], we have

$$\mathcal{R}_1\leq C\Delta t+\varepsilon_1\mathbb{E}\left[\sum_{n=1}^{m}|||\theta^n|||^2\Delta t\right], \tag{4.29}$$

and

$$\mathcal{R}_3\leq C\Delta t+\varepsilon_2\mathbb{E}\left[\sum_{n=0}^{m-1}\|\theta^{n+1}-\theta^n\|^2\right]. \tag{4.30}$$

For the term $\mathcal{R}_2$, applying the Cauchy–Schwarz inequality, Young's inequality and Lemma 2.3 gives

$$\begin{aligned}\mathcal{R}_2\leq&\mathbb{E}\left[\sum_{n=0}^{m-1}\int_{t_n}^{t_{n+1}}\|f(u(t_{n+1}))-f(u(s))\|\|\theta^{n+1}\|\mathrm{d}s\right]\\\leq&C\sum_{n=0}^{m-1}\int_{t_n}^{t_{n+1}}\mathbb{E}\left[\|f(u(t_{n+1}))-f(u(s))\|^2\right]\mathrm{d}s+C\mathbb{E}\left[\sum_{n=0}^{m-1}\int_{t_n}^{t_{n+1}}\|\theta^{n+1}\|^2\mathrm{d}s\right]\\\leq&C\Delta t+C\Delta t\mathbb{E}\left[\sum_{n=0}^{m-1}\|\theta^{n+1}\|^2\right].\end{aligned} \tag{4.31}$$

Combining (4.29)-(4.31) completes the proof. □

Lemma 4.10 ([46])**.** *Under the same conditions of Lemma* 2.1*, the following estimate holds:*

$$\mathbb{E}\left[\sum_{n=0}^{m-1}\|\rho^{n+1}-\rho^n\|^2\right]\leq Ch^{2\min\{r+1,\kappa\}}. \tag{4.32}$$

Lemma 4.11 ([46]). *Under the same conditions of Lemma* 2.2*, we have the following estimate*

$$\mathbb{E}\left[\sum_{n=0}^{m-1}\left(\mathbb{E}\left[\rho^{n+1}-\rho^n|\mathcal{F}_{t_n}\right],\theta^n\right)\right]\leq Ch^{2\min\{r+1,\kappa\}}+C\mathbb{E}\left[\sum_{n=0}^{m-1}\|\theta^n\|^2\Delta t\right]. \tag{4.33}$$

Theorem 4.2. *Suppose Assumptions* 2.1 *and* 2.2 *hold, and*

$$u\in C_{\mathbb{F}}\left([0,T];L^6\left(\Omega,H^\kappa(D)\right)\right)\bigcap L^6_{\mathbb{F}}\left((0,T);H^{\kappa+1}(D)\right)\bigcap L^2_{\mathbb{F}}\left((0,T);H^{2+\kappa}(D)\right),\quad \kappa\geq 2.$$

Then there exists a constant C independent of the mesh size h and the time step Δt*, such that*

$$\sup_{0\leq n\leq\mathbb{M}}\mathbb{E}\left[\|\theta^m\|^2\right]+C_a\mathbb{E}\left[\sum_{n=0}^{\mathbb{M}}|||\theta^n|||^2\Delta t\right]\leq C\Delta t+Ch^{2\min\{r+1,\kappa\}}. \tag{4.34}$$

Proof. By substituting (4.28), (4.32), and (4.33) into (4.17), we deduce

$$\begin{aligned}
&\frac{1}{2}\mathbb{E}\left[\|\theta^m\|^2\right]+\frac{1}{4}\mathbb{E}\left[\sum_{n=0}^{m-1}\|\theta^{n+1}-\theta^n\|^2\right]+C_a\mathbb{E}\left[\sum_{n=1}^{m}|||\theta^n|||^2\Delta t\right]\\
&\leq Ch^{2\min\{r+1,\kappa\}}+C\Delta t+C\mathbb{E}\left[\sum_{n=0}^{m-1}\|\rho^{n+1}\|^2\Delta t\right]+C\mathbb{E}\left[\sum_{n=0}^{m-1}\|\rho^n\|^2\Delta t\right]\\
&\quad+C\mathbb{E}\left[\sum_{n=0}^{m-1}\|\theta^n\|^2\Delta t\right]+C\mathbb{E}\left[\sum_{n=0}^{m-1}\|\theta^{n+1}\|^2\Delta t\right]\\
&\quad+\varepsilon_1\mathbb{E}\left[\sum_{n=1}^{m}|||\theta^n|||^2\Delta t\right]+\varepsilon_2\mathbb{E}\left[\sum_{n=0}^{m-1}\|\theta^{n+1}-\theta^n\|^2\right].
\end{aligned} \tag{4.35}$$

Choosing Δt, ε_1, and ε_2 such that $\frac{1}{2}-C\Delta t>0$, $\varepsilon_1=\frac{1}{2}C_a$, and $\frac{1}{4}-\varepsilon_2>0$ gives

$$\begin{aligned}
&\mathbb{E}\left[\|\theta^m\|^2\right]+C_a\mathbb{E}\left[\sum_{n=1}^{m}|||\theta^n|||^2\Delta t\right]\\
&\leq Ch^{2\min\{r+1,\kappa\}}+C\Delta t+C\mathbb{E}\left[\sum_{n=0}^{m}\|\theta^n\|^2\Delta t\right].
\end{aligned} \tag{4.36}$$

With the discrete Gronwall inequality in Lemma 4.6, we complete the proof. □

4.4 Proof of Theorem 4.1

In this subsection, we are going to prove our main result concerning the strong optimal error estimates for the proposed fully discrete Scheme 3.1.

Proof. Note that $e^n = u_h^n - u(t_n) = \theta^n - \rho^n$. With the help of the triangle inequality, we achieve that

$$\begin{aligned}
&\mathbb{E}\left[\|e^n\|^2\right] + h^2 C\mathbb{E}\left[\sum_{n=0}^{\mathbb{M}} |||e^n|||^2 \Delta t\right] \\
=&\mathbb{E}\left[\|\theta^n - \rho^n\|^2\right] + h^2 C\mathbb{E}\left[\sum_{n=0}^{\mathbb{M}} |||\theta^n - \rho^n|||^2 \Delta t\right] \\
\leq& 2\mathbb{E}\left[\|\theta^n\|^2\right] + 2\mathbb{E}\left[\|\rho^n\|^2\right] + 2h^2 C\mathbb{E}\left[\sum_{n=0}^{\mathbb{M}} |||\theta^n|||^2 \Delta t\right] \\
&+ 2h^2 C\mathbb{E}\left[\sum_{n=0}^{\mathbb{M}} |||\rho^n|||^2 \Delta t\right].
\end{aligned} \tag{4.37}$$

Based on Lemma 4.2 and Theorem 4.2, it follows that

$$\begin{aligned}
&\mathbb{E}\left[\|e^n\|^2\right] + h^2 C\mathbb{E}\left[\sum_{n=0}^{\mathbb{M}} |||e^n|||^2 \Delta t\right] \\
\leq& C\Delta t + Ch^{2\min\{r+1,\kappa\}} + h^2 C\mathbb{E}\left[\|\rho^n\|^2\right] + h^2 C\mathbb{E}\left[\sum_{n=0}^{\mathbb{M}} |||\rho^n|||^2 \Delta t\right] \\
\leq& C\Delta t + Ch^{2\min\{r+1,\kappa\}}.
\end{aligned} \tag{4.38}$$

This result gives the desired error bound in Theorem 4.1. □

5 Numerical results

In this section, we first present the accuracy testing to support the theoretical results and then provide the mergence of four bubbles and the phase separation tests to demonstrate the effectiveness of Scheme 3.1 for solving the SAC equation (1.1)-(1.3).

Convergence tests

The computational domain in the following tests is chosen to be a unit square $D = [0,1]^2$. The numerical tests are performed on a sequence of discretizations with respect to the time step Δt in time and the spatial mesh size h in space. Since the exact solution of (1.1)-(1.3) is unknown, we approximate the stochastic L^2 error by the average of a family of path-wise solutions with $\{\omega_i \in \Omega\}_{i=1}^M$ as

$$(e[u_h^n])^2 := \mathbb{E}[\|u(t_n) - u_h^n\|^2] \approx \frac{1}{M}\sum_{i=1}^{M} \|u_h^n(\omega_i) - u_{\text{ref}}^n(\omega_i)\|^2, \tag{5.1}$$

where $\{u_{\text{ref}}^n(\omega_i)\}$ refer to the reference solutions and are specified on finest mesh.

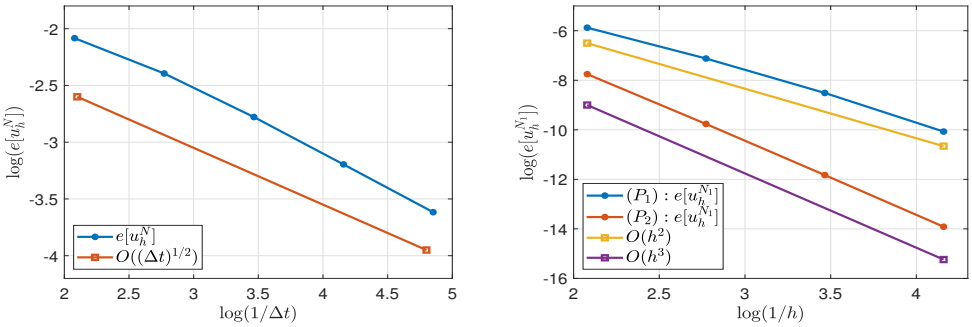

Figure 1: Errors and convergence rates of Case 1.

The configurations of the numerical tests are summarized as follows. The number of samples $\{\omega_i\}_{i=1}^M$ is taken as $M=1000$. For the temporal convergence tests, we first generate M discrete $W(t)$ with sufficiently small $\Delta t_{\text{ref}}=1/2^{10}$, see [24]. The discontinuous Galerkin Scheme 3.1 equipped with P_2 discontinuous polynomial space on $\mathcal{T}_h$ and $h=1/2^6$ is checked on a sequence of time discretizations with time step $\Delta t=1/2^k$,$k=$ 3,4,5,6,7. For the spatial convergence tests, we take time step $\Delta t=10^{-10}$. We then employ a sequence of uniform triangulations $\{\mathcal{T}_h\}$ in space with $h=1/2^k$, $k=2,3,4,5,6$ and a fixed small time step $\Delta t=10^{-10}$. The reference solution u_{ref} is taken as the numerical solution on the finest discretization with $h_{\text{ref}}=1/2^7$ and $\Delta t_{\text{ref}}=10^{-10}$. The discontinuous Galerkin Scheme 3.1 with P_1 and P_2 discontinuous polynomial bases is further carried out to confirm the accuracy, respectively.

• CASE 1. In the first test, we consider the following stochastic Allen-Cahn equation with $\epsilon=1$, in which the multiplicative noise term consists of the sine function and one dimensional standard Wiener process as

$$\mathrm{d}u-\Delta u\mathrm{d}t=f(u)\mathrm{d}t+\sin(u)\mathrm{d}W \tag{5.2}$$

with an initial condition $u(0,x)=\sin^2(\pi x)\sin^2(\pi y)$.

We present the computational results of Case 1 in Fig. 1 which illustrates the convergence errors and rates. The left plot of Fig. 1 shows time convergence tests of Scheme 3.1 at $t_N=1$ from which we see that the optimal convergence rates is 0.5 in time. The space convergence information at $t_N=1000\times10^{-10}$ is given in the right of Fig. 1. We see that the L^2 optimal convergence rates 2, 3 for P_1, P_2 discontinuous polynomial bases in space are both numerically obtained, respectively. The computational results are what we expected.

• CASE 2. To further verify the accuracy of Scheme 3.1, in this test, we set the multiplicative noise comprised of the sigmoid function as

$$\mathrm{d}u-\Delta u\mathrm{d}t=f(u)\mathrm{d}t+\frac{2}{1+e^{-u}}\mathrm{d}W. \tag{5.3}$$

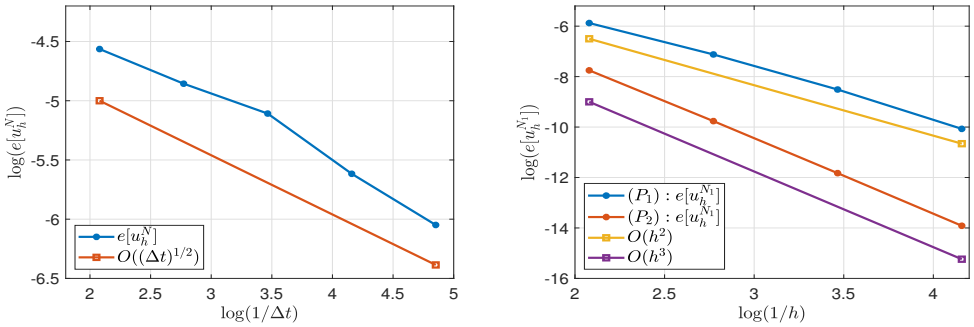

Figure 2: Errors and Convergence rates of Case 2.

The initial condition is further chosen as a polynomial function $u(0,x)=10x^2y^2(1-x)^2(1-y)^2$ and the other settings are the same as those in Case 1.

It can be checked that the sigmoid function satisfies the requirement of Assumption 2.1 in our theoretical analysis. The computational results of Case 2 are given in Fig. 2. From Fig. 2, we see that the spatial convergence rates are 2, 3 for the P_1 and P_2 discontinuous polynomial bases, respectively. The optimal order of convergence 0.5 in time is also numerically obtained. In conclusion, the simulation results of Cases 1 and 2 are both consistent with our theoretical results and further verify our theoretical result in Theorem 4.1.

Mergence of four bubbles

Referring to [35, 40], we consider the stochastic Allen-Cahn equation on $D=[0,1]^2$ as

$$\mathrm{d}u-\Delta u\mathrm{d}t=\frac{1}{\epsilon^2}(1-u^2)u\mathrm{d}t+\frac{\gamma}{\epsilon^2}(1-u^2)u\mathrm{d}W, \tag{5.4}$$

where the diffusion coefficient $\epsilon=0.02$ and the initial condition is given as

$$\begin{aligned}u_0(x,y)=&-\tanh(((x-0.3)^2+y^2-0.2^2)/\epsilon)\tanh(((x-0.3)^2+y^2-0.2^2)/\epsilon)\\&\times\tanh((x^2+(y-0.3)^2-0.2^2)/\epsilon)\tanh((x^2+(y-0.3)^2-0.2^2)/\epsilon).\end{aligned}$$

To examine the influence of the noise perturbation to (5.4), we set four different $\gamma=0, 1.8\times10^{-2}, 1.4\times10^{-2}$ and 1.0×10^{-2}, respectively. To carry out the tests, the P_2 discontinuous Galerkin space is used with 4096 uniform triangle elements and time step $\Delta t=10^{-4}$. For the case with $\gamma=0$, model (5.4) reduces to the deterministic Allen-Cahn equation. Fig. 3 illustrates the simulation results at different time instants $\bar{t}_1=0$, $\bar{t}_2=7\times10^{-3}$, $\bar{t}_3=9\times10^{-3}$ and $\bar{t}_4=5\times10^{-2}$. From Fig. 3, we see that computational results are consistent with those in [35].

The stochastic cases are presented in Fig. 4 with Monte Carlo simulation number $M=100$. The evolution results shown in Figs. 4(a)-4(d) are obtained with $\bar{\gamma}_1=1.8\times10^{-2}$

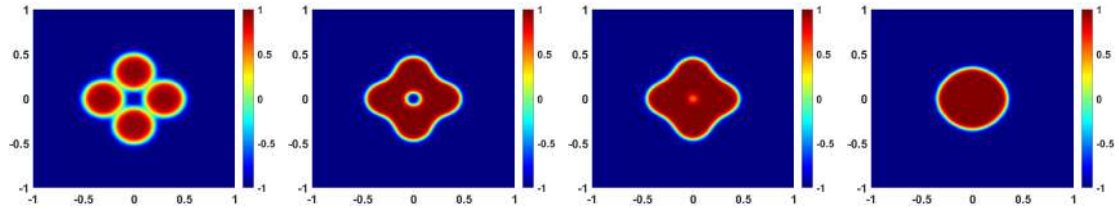

(a) $t=\bar{t}_1$ (b) $t=\bar{t}_2$ (c) $t=\bar{t}_3$ (d) $t=\bar{t}_4$

Figure 3: Evolution of the deterministic AC for the mergence of four bubbles.

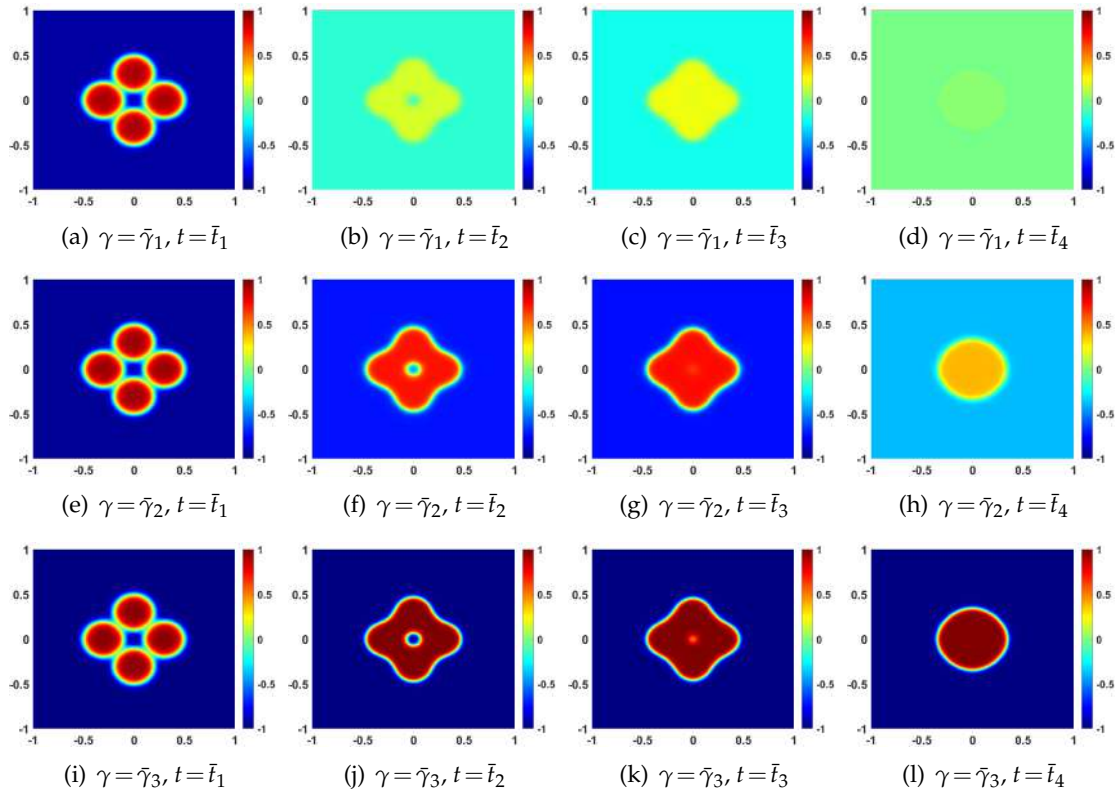

(a) $\gamma=\bar{\gamma}_1, t=\bar{t}_1$ (b) $\gamma=\bar{\gamma}_1, t=\bar{t}_2$ (c) $\gamma=\bar{\gamma}_1, t=\bar{t}_3$ (d) $\gamma=\bar{\gamma}_1, t=\bar{t}_4$

(e) $\gamma=\bar{\gamma}_2, t=\bar{t}_1$ (f) $\gamma=\bar{\gamma}_2, t=\bar{t}_2$ (g) $\gamma=\bar{\gamma}_2, t=\bar{t}_3$ (h) $\gamma=\bar{\gamma}_2, t=\bar{t}_4$

(i) $\gamma=\bar{\gamma}_3, t=\bar{t}_1$ (j) $\gamma=\bar{\gamma}_3, t=\bar{t}_2$ (k) $\gamma=\bar{\gamma}_3, t=\bar{t}_3$ (l) $\gamma=\bar{\gamma}_3, t=\bar{t}_4$

Figure 4: The averaged evolution of stochastic Allen-Cahn equations with different $\bar{\gamma}_1=1.8\times10^{-2}$, $\bar{\gamma}_2=1.4\times10^{-2}$ and $\bar{\gamma}_3=10^{-2}$ for the mergence of four bubbles.

followed by $\bar{\gamma}_2=1.4\times10^{-2}$ and $\bar{\gamma}_3=10^{-2}$. Fig. 4 shows that the initial states with four bubbles are gradually merging into a single bubble with time evolution for the three different cases. The computational results also show that the magnitude of stochastic phase field decays faster with larger noise perturbation. From Figs. 4(i)-4(l), we see that the stochastic Allen-Cahn model (5.4) approaches to the deterministic cases with sufficiently small noise perturbation.

Phase separation

The deterministic Allen-Cahn equation is commonly used as coarsening dynamics for simulating certain phase separation [35]. To see the phenomenon of the phase separation related to the stochastic Allen-Cahn equation, by referring to [40], we consider the stochastic Allen-Cahn equation (5.4) with an initial condition given as $u_0(x,y) = 0.1 \times \text{rand(x,y)}$ where 'rand' is a uniform random generator in $[-1,1]$. In all the following computation, the initial condition u_0 is fixed and depicted in Fig. 5. We further set the parameters $\epsilon = 10^{-2}$, $\Delta t = 10^{-5}$. The domain $D = [0,1]^2$ is divided into 4098 uniform triangles and the P_2 discontinuous Galerkin space is used in the simulations.

The deterministic Allen-Cahn equation with $\gamma = 0$ in (5.4) is first investigated as reference states. The related simulation results at time instants $\tilde{t}_1 = 10^{-4}$, $\tilde{t}_2 = 5\times 10^{-4}$, $\tilde{t}_3 = 8\times 10^{-4}$ and $\tilde{t}_4 = 10^{-3}$ for the deterministic case are listed in Fig. 6. As seen from Fig. 6, the phase separation patterns with the time evolution are gradually apparent from Fig. 6(a) to Fig. 6(d).

To investigate the coarsening dynamics of the stochastic Allen-Cahn equation, four sets of numerical tests are performed with different γ, i.e., $\tilde{\gamma}_1 = 10^{-1}$, $\tilde{\gamma}_2 = 10^{-2}$, $\tilde{\gamma}_3 = 5\times 10^{-3}$ and $\tilde{\gamma}_4 = 10^{-3}$ in (5.4) and $M = 100$ simulations are then done for each case. Figs. 7 and 8 show the evolution of the averaged phase states. As can be seen for the case with

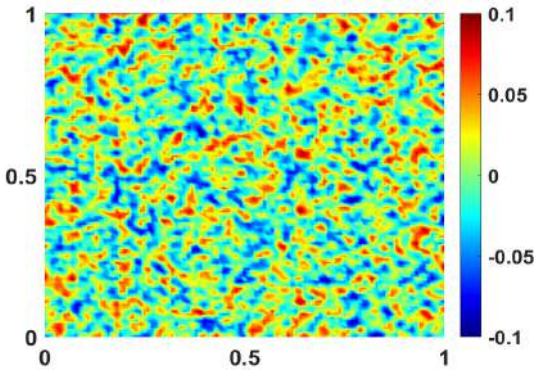

Figure 5: The initial condition.

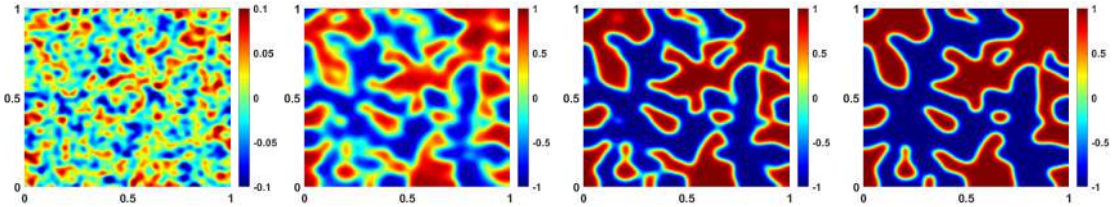

(a) $t = \tilde{t}_1$ (b) $t = \tilde{t}_2$ (c) $t = \tilde{t}_3$ (d) $t = \tilde{t}_4$

Figure 6: Evolution of the deterministic Allen-Cahn equation for phase separation.

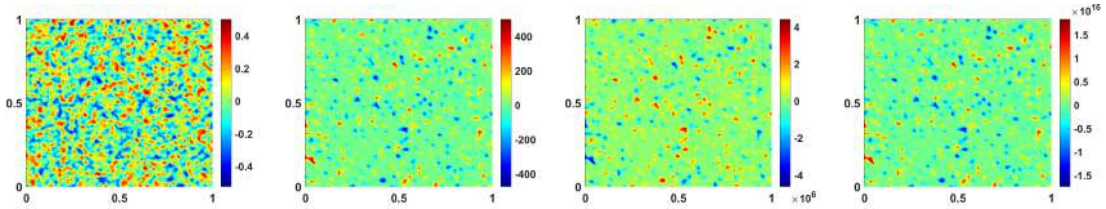

(a) $t=\tilde{t}_1$ (b) $t=\tilde{t}_2$ (c) $t=\tilde{t}_3$ (d) $t=\tilde{t}_4$

Figure 7: The averaged evolution of stochastic Allen-Cahn equation with $\tilde{\gamma}_1=10^{-1}$ for phase separation.

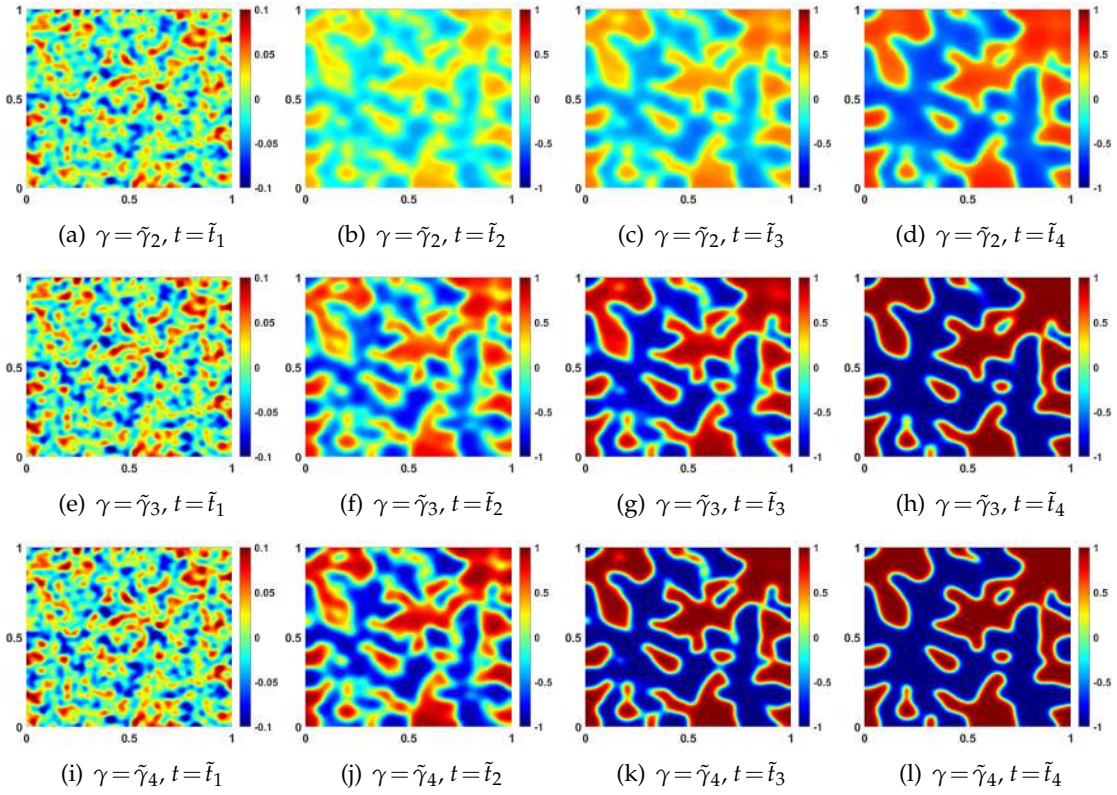

(a) $\gamma=\tilde{\gamma}_2, t=\tilde{t}_1$ (b) $\gamma=\tilde{\gamma}_2, t=\tilde{t}_2$ (c) $\gamma=\tilde{\gamma}_2, t=\tilde{t}_3$ (d) $\gamma=\tilde{\gamma}_2, t=\tilde{t}_4$

(e) $\gamma=\tilde{\gamma}_3, t=\tilde{t}_1$ (f) $\gamma=\tilde{\gamma}_3, t=\tilde{t}_2$ (g) $\gamma=\tilde{\gamma}_3, t=\tilde{t}_3$ (h) $\gamma=\tilde{\gamma}_3, t=\tilde{t}_4$

(i) $\gamma=\tilde{\gamma}_4, t=\tilde{t}_1$ (j) $\gamma=\tilde{\gamma}_4, t=\tilde{t}_2$ (k) $\gamma=\tilde{\gamma}_4, t=\tilde{t}_3$ (l) $\gamma=\tilde{\gamma}_4, t=\tilde{t}_4$

Figure 8: The averaged evolution of stochastic Allen-Cahn equations with different $\tilde{\gamma}_2=10^{-2}$, $\tilde{\gamma}_3=5\times10^{-3}$ and $\tilde{\gamma}_4=10^{-3}$ for phase separation.

$\tilde{\gamma}_1=10^{-1}$ in Fig. 7, the computational solutions of the stochastic Allen-Cahn equation are going to blow up with time evolution, which implies that the larger perturbation of the noise term will completely destroy the properties of the original deterministic case. Then we downgrade the magnitude of the noise terms by setting γ from 10^{-2} to 10^{-3}. The correspondingly computational results are depicted in Fig. 8. Figs. 8(a)-8(d) illus-

trate the phase states with $\tilde{\gamma}_2 = 10^{-2}$, from which it can be seen that the phase separation boundaries are relatively fuzzy. Fortunately, the outline of the phase separation can be roughly distinct. As we further decrease the parameter γ to 5×10^{-3} and 10^{-3}, the migration of the phase boundaries can be apparently observed as shown in Figs. 8(e)-8(l), which means that the stochastic Allen-Cahn equation with small noise perturbation can keep the properties of coarsening dynamics as the case of the deterministic Allen-Cahn equation.

6 Conclusions

In this work, a fully discrete SIPG scheme for stochastic Allen-Cahn equation driven by multiplicative noise is rigorously studied. The space discretization is performed by symmetric interior penalty discontinuous Galerkin finite element method and the implicit Euler method is used for temporal discretization. Error estimates for the proposed numerical scheme are established and optimal strong convergence rates in both space and time are recovered. The numerical results concord well with our theoretical findings. Based on the techniques developed in this paper, the other types of DG methods such as NIPG, IIPG, etc., can be further studied.

Acknowledgments

This research is partially supported by the National Natural Science Foundation of China (Grant Nos. 12371398, 12071261, 11901565, 12001325, 12131014).

References

[1] Samuel M. Allen and John W. Cahn, *A microscopic theory for antiphase boundary motion and its application to antiphase domain coarsening*, Acta Metallurgica **27** (1979), no. 6, 1085–1095.

[2] Lehel Banjai, Gabriel Lord, and Jeta Molla, *Strong convergence of a Verlet integrator for the semilinear stochastic wave equation*, SIAM J. Numer. Anal. **59** (2021), no. 4, 1976–2003. MR 4285774

[3] Dirk Blömker and Minoo Kamrani, *Numerically computable a posteriori-bounds for the stochastic Allen-Cahn equation*, BIT **59** (2019), no. 3, 647–673. MR 4001780

[4] Charles-Edouard Bréhier, Jianbo Cui, and Jialin Hong, *Strong convergence rates of semidiscrete splitting approximations for the stochastic Allen-Cahn equation*, IMA J. Numer. Anal. **39** (2019), no. 4, 2096–2134. MR 4019051

[5] Charles-Edouard Bréhier and Ludovic Goudenège, *Analysis of some splitting schemes for the stochastic Allen-Cahn equation*, Discrete Contin. Dyn. Syst. Ser. B **24** (2019), no. 8, 4169–4190. MR 3986273

[6] Susanne C. Brenner, *Poincaré–friedrichs inequalities for piecewise h1 functions*, SIAM Journal on Numerical Analysis **41** (2003), no. 1, 306–324.

[7] Susanne C. Brenner and L. Ridgway Scott, *The Mathematical Theory of Finite Element Methods*, third ed., Texts in Applied Mathematics, vol. 15, Springer, New York, 2008. MR 2373954

[8] Zdzislaw Brzeźniak, Erich Carelli, and Andreas Prohl, *Finite-element-based discretizations of the incompressible Navier-Stokes equations with multiplicative random forcing*, IMA J. Numer. Anal. **33** (2013), no. 3, 771–824. MR 3081484

[9] Meng Cai, Siqing Gan, and Xiaojie Wang, *Weak convergence rates for an explicit full-discretization of stochastic Allen-Cahn equation with additive noise*, J. Sci. Comput. **86** (2021), no. 3, Paper No. 34, 30. MR 4200962

[10] Yanzhao Cao, Ran Zhang, and Kai Zhang, *Finite element and discontinuous Galerkin method for stochastic Helmholtz equation in two- and three-dimensions*, J. Comput. Math. **26** (2008), no. 5, 702–715. MR 2444727

[11] ———, *Finite element method and discontinuous Galerkin method for stochastic scattering problem of Helmholtz type in* $\mathbb{R}^d$ $(d=2,3)$, Potential Anal. **28** (2008), no. 4, 301–319. MR 2403284

[12] Chuchu Chen, *A symplectic discontinuous Galerkin full discretization for stochastic Maxwell equations*, SIAM J. Numer. Anal. **59** (2021), no. 4, 2197–2217. MR 4297827

[13] Chuchu Chen, Jialin Hong, and Lihai Ji, *Mean-square convergence of a symplectic local discontinuous Galerkin method applied to stochastic linear Schrödinger equation*, IMA J. Numer. Anal. **37** (2017), no. 2, 1041–1065. MR 3649434

[14] Pao-Liu Chow, *Stochastic Partial Differential Equations*, second ed., Advances in Applied Mathematics, CRC Press, Boca Raton, FL, 2015. MR 3288853

[15] Philippe G. Ciarlet, *The finite element method for elliptic problems*, Classics in Applied Mathematics, vol. 40, Society for Industrial and Applied Mathematics (SIAM), Philadelphia, PA, 2002, Reprint of the 1978 original [North-Holland, Amsterdam; MR0520174 (58 #25001)]. MR 1930132

[16] Bernardo Cockburn, George E. Karniadakis, and Chi-Wang Shu, *The development of discontinuous Galerkin methods*, Discontinuous Galerkin methods (Newport, RI, 1999), Lect. Notes Comput. Sci. Eng., vol. 11, Springer, Berlin, 2000, pp. 3–50. MR 1842161

[17] Jianbo Cui and Jialin Hong, *Strong and weak convergence rates of a spatial approximation for stochastic partial differential equation with one-sided Lipschitz coefficient*, SIAM J. Numer. Anal. **57** (2019), no. 4, 1815–1841. MR 3984308

[18] Daniele Antonio Di Pietro and Alexandre Ern, *Mathematical Aspects of Discontinuous Galerkin Methods*, Mathématiques & Applications (Berlin) [Mathematics & Applications], vol. 69, Springer, Heidelberg, 2012. MR 2882148

[19] Vít Dolejší and Miloslav Feistauer, *Discontinuous Galerkin Method*, Springer Series in Computational Mathematics, vol. 48, Springer, Cham, 2015, Analysis and applications to compressible flow. MR 3363720

[20] Alexandre Ern and Jean-Luc Guermond, *Theory and Practice of Finite Elements*, Applied Mathematical Sciences, vol. 159, Springer-Verlag, New York, 2004. MR 2050138

[21] Xiaobing Feng, Yukun Li, and Yi Zhang, *Finite element methods for the stochastic Allen-Cahn equation with gradient-type multiplicative noise*, SIAM J. Numer. Anal. **55** (2017), no. 1, 194–216. MR 3600370

[22] ———, *Strong convergence of a fully discrete finite element method for a class of semilinear stochastic partial differential equations with multiplicative noise*, J. Comput. Math. **39** (2021), no. 4, 574–598. MR 4319577

[23] Vivette Girault and Pierre-Arnaud Raviart, *Finite Element Methods for Navier-Stokes Equations*, Springer Series in Computational Mathematics, vol. 5, Springer-Verlag, Berlin, 1986, Theory and algorithms. MR 851383

[24] Max D. Gunzburger and Wenju Zhao, *Descriptions, discretizations, and comparisons of time/space colored and white noise forcings of the Navier-Stokes equations*, SIAM J. Sci. Comput.

41 (2019), no. 4, A2579–A2602. MR 3992504
[25] István Gyöngy and Annie Millet, *Rate of convergence of implicit approximations for stochastic evolution equations*, Stochastic Differential Equations: Theory and Applications, Interdiscip. Math. Sci., vol. 2, World Sci. Publ., Hackensack, NJ, 2007, pp. 281–310. MR 2393581
[26] Jialin Hong, Baohui Hou, and Liying Sun, *Energy-preserving fully-discrete schemes for nonlinear stochastic wave equations with multiplicative noise*, J. Comput. Phys. **451** (2022), Paper No. 110829, 20. MR 4362830
[27] Bülent Karasözen, Murat Uzunca, Ayşe Sariaydin-Filibelioğlu, and Hamdullah Yücel, *Energy stable discontinuous Galerkin finite element method for the Allen-Cahn equation*, Int. J. Comput. Methods **15** (2018), no. 3, 1850013, 26. MR 3790582
[28] Mihály Kovács, Stig Larsson, and Fredrik Lindgren, *On the backward Euler approximation of the stochastic Allen-Cahn equation*, J. Appl. Probab. **52** (2015), no. 2, 323–338. MR 3372078
[29] ———, *On the discretisation in time of the stochastic Allen-Cahn equation*, Math. Nachr. **291** (2018), no. 5-6, 966–995. MR 3795566
[30] Raphael Kruse and Rico Weiske, *The BDF2-Maruyama method for the stochastic Allen-Cahn equation with multiplicative noise*, J. Comput. Appl. Math. **419** (2023), Paper No. 114634, 13. MR 4475984
[31] Chen Li, Ruibin Qin, Ju Ming, and Zhongming Wang, *A discontinuous Galerkin method for stochastic Cahn-Hilliard equations*, Comput. Math. Appl. **75** (2018), no. 6, 2100–2114. MR 3775106
[32] Yunzhang Li, Chi-Wang Shu, and Shanjian Tang, *A discontinuous Galerkin method for stochastic conservation laws*, SIAM J. Sci. Comput. **42** (2020), no. 1, A54–A86. MR 4048017
[33] ———, *An ultra-weak discontinuous Galerkin method with implicit-explicit time-marching for generalized stochastic KdV equations*, J. Sci. Comput. **82** (2020), no. 3, Paper No. 61, 36. MR 4066632
[34] ———, *A local discontinuous Galerkin method for nonlinear parabolic SPDEs*, ESAIM Math. Model. Numer. Anal. **55** (2021), no. suppl., S187–S223. MR 4221304
[35] Hong-lin Liao, Tao Tang, and Tao Zhou, *On energy stable, maximum-principle preserving, second-order BDF scheme with variable steps for the Allen-Cahn equation*, SIAM J. Numer. Anal. **58** (2020), no. 4, 2294–2314. MR 4134034
[36] Chen Liu and Béatrice Rivière, *A priori error analysis of a discontinuous galerkin method for cahn–hilliard–navier–stokes equations*, CSIAM Transactions on Applied Mathematics **1** (2020), no. 1, 104–141.
[37] Zhihui Liu and Zhonghua Qiao, *Strong approximation of monotone stochastic partial differential equations driven by multiplicative noise*, Stoch. Partial Differ. Equ. Anal. Comput. **9** (2021), no. 3, 559–602. MR 4297233
[38] Ting Ma and Rong Chan Zhu, *Convergence rate for Galerkin approximation of the stochastic Allen-Cahn equations on 2D torus*, Acta Math. Sin. (Engl. Ser.) **37** (2021), no. 3, 471–490. MR 4229518
[39] Ananta K. Majee and Andreas Prohl, *Optimal strong rates of convergence for a space-time discretization of the stochastic Allen-Cahn equation with multiplicative noise*, Comput. Methods Appl. Math. **18** (2018), no. 2, 297–311. MR 3776047
[40] Carl Mueller, Leonid Mytnik, and Jeremy Quastel, *Effect of noise on front propagation in reaction-diffusion equations of KPP type*, Invent. Math. **184** (2011), no. 2, 405–453. MR 2793860
[41] Ruisheng Qi and Xiaojie Wang, *Optimal error estimates of Galerkin finite element methods for stochastic Allen-Cahn equation with additive noise*, J. Sci. Comput. **80** (2019), no. 2, 1171–1194. MR 3977202
[42] Béatrice Rivière, *Discontinuous Galerkin methods for solving elliptic and parabolic equations*, Frontiers in Applied Mathematics, vol. 35, Society for Industrial and Applied Mathemat-

ics (SIAM), Philadelphia, PA, 2008, Theory and implementation. MR 2431403

[43] Jiawei Sun, Chi-Wang Shu, and Yulong Xing, *Multi-symplectic discontinuous Galerkin methods for the stochastic Maxwell equations with additive noise*, J. Comput. Phys. **461** (2022), Paper No. 111199, 30. MR 4410964

[44] _____, *Discontinuous Galerkin methods for stochastic Maxwell equations with multiplicative noise*, ESAIM Math. Model. Numer. Anal. **57** (2023), no. 2, 841–864. MR 4567994

[45] Xiaojie Wang, *An efficient explicit full-discrete scheme for strong approximation of stochastic Allen-Cahn equation*, Stochastic Process. Appl. **130** (2020), no. 10, 6271–6299. MR 4140034

[46] Xu Yang, Weidong Zhao, and Wenju Zhao, *Strong optimal error estimates of discontinuous Galerkin method for multiplicative noise driving nonlinear SPDEs*, Numer. Methods Partial Differential Equations **39** (2023), no. 3, 2073–2095. MR 4570537

[47] Li Zhou and Yunzhang Li, *An LDG method for stochastic Cahn-Hilliard type equation driven by general multiplicative noise involving second-order derivative*, Commun. Comput. Phys. **31** (2022), no. 2, 516–547. MR 4371451